Appl Magn Reson (2017) 48:559–569
DOI 10.1007/s00723-017-0884-y

Applied Magnetic Resonance

ORIGINAL PAPER

Using Terahertz Waves to Identify the Presence of Goethite via Antiferromagnetic Resonance

S. G. Chou[1] · P. E. Stutzman[2] · V. Provenzano[3] · R. D. McMichael[4] · J. Surek[5] · S. Wang[6] · D. F. Plusquellic[7] · E. J. Garboczi[8]

Received: 15 December 2016 / Published online: 24 April 2017

Abstract Virtually every corrosion detection method reports only the presence of a material phase that denotes probable corrosion, not its spectral signature. A signature specific to the type of iron oxide corrosion product would not only confirm the presence of corrosion but also provide insight into the environment of its formation. To identify the unique spectral signature of a commonly occurring corrosion product, goethite (α-FeOOH), we performed high-resolution terahertz (THz) absorption loss measurements on a polycrystalline mineral sample of goethite, scanning from 0.045 to 1.5 THz. We report two distinct temperature-dependent absorption peaks that extend from 4.2 to 425 K. By combining X-ray diffraction and

✉ E. J. Garboczi
edward.garboczi@nist.gov

[1] Office of Pharmaceutical Quality, Center for Drug Evaluation and Research, U. S. Food and Drug Administration, U. S. Department of Health and Human Services, Silver Spring, MD 20903, USA

[2] Engineering Laboratory, National Institute of Standards and Technology, Gaithersburg, MD 20899, USA

[3] Material Measurement Laboratory, National Institute of Standards and Technology, Gaithersburg, MD 20899, USA

[4] Center for Nanoscience and Technology, National Institute of Standards and Technology, Gaithersburg, MD 20899, USA

[5] Communications Technology Laboratory, National Institute of Standards and Technology, Boulder, CO 80305, USA

[6] Office of Material Technology, Maryland Department of Transportation, Hanover, MD 20176, USA

[7] Physical Measurement Laboratory, National Institute of Standards and Technology, Boulder, CO 80305, USA

[8] Material Measurement Laboratory, National Institute of Standards and Technology, Boulder, CO 80305, USA

magnetic characterization on this large crystallite-sized goethite sample, we derived a Neél transition temperature of 435 K, below which the sample is antiferromagnetic. We interpret these absorption peaks as magnon transitions of the antiferromagnetic resonances, allowing precise identification of goethite, a common iron corrosion product and geological mineral, via two terahertz absorption peaks over this temperature range. This measurement technique has the potential for detecting iron-bearing oxides originating from corrosion occurring underneath layers of polymeric products and other protective coatings that can be easily penetrated by electromagnetic waves with frequencies on the order of 1 THz. Furthermore, the combined X-ray and magnetic characterization of this sample, which had a large crystallite size, also improved the previously established relationship between the Néel transition temperature and the inverse mean crystallite dimension in the [111] direction. Our results provide end-case peaks which, compared with goethite samples of smaller crystallite size and purity, will enable the extension of this non-destructive evaluation technique to real corrosion applications.

1 Introduction

Goethite (α-FeOOH) is one of the most prevalent iron oxide minerals on the Earth's surface [1–3]. It is also grown for industrial purposes as acicular submicrometer particles [1]. Goethite is one of the most abundant constituents in corrosion products of steel formed in humid environments [4, 5] and can absorb metals such as gallium, nickel, and arsenic [6]. Goethite is antiferromagnetic, with Fe^{3+}-centered spins that anti-pair through oxygen and hydroxyl ligands by superexchange. This antiferromagnetic pairing of spins up to a Néel transition temperature (T_N) around 400 K has been clearly established for goethite crystals by inelastic neutron scattering [6–9].

The use of THz electromagnetic radiation to detect absorptions associated with the antiferromagnetic structure of goethite and, in our previous work, hematite [10] was motivated by a desire to go beyond the U.S. national need for early detection of iron corrosion [11–14] via non-destructive evaluation (NDE) and move toward specific identification of these common iron corrosion species with a technique able to penetrate concrete, polymer, and other protective coatings [15]. The antiferromagnetic (AFM) absorption that we observed in hematite is near 100 GHz [10] in the temperature range just below water freezing, making it suitable for detecting hematite corrosion products of reinforcing steel under $\sim$50 mm thickness of cover concrete in a cold winter [16]. The goethite absorptions we report here occur at roughly twice and four times the frequency of our hematite resonances. Because penetration depth decreases with the frequency of the THz excitation energy, the current results are more applicable for identifying goethite-based corrosion products embedded under polymer and polymer composite coatings (e.g., pipe insulation in a factory). It would be very difficult with today's technology to detect these waves through $\sim$50 mm of concrete.

As a part of our magnetic characterization, we found the Néel temperature for our crystal sample to be about 435 K, implying large crystallite size and fewer lattice imperfections when compared to previous studies. To further establish the

relationship between crystallite size and Neel transition temperature, we decided to extend the plot provided in [17] with this additional temperature point.

The essence of this study is our observation of two optical absorption peaks, whose positions are recorded as a function of temperature in a good quality goethite polycrystalline mineral sample. The positions of these transitions were recorded for the goethite crystal in its antiferromagnetic phase with temperature spanning from 4.2 up to 425 K, just below the Néel transition temperature (435 K), excited using a high-precision terahertz optical source generating excitation energies ranging from 0.045 to 1.5 THz (1.5 and 50 cm^{-1}). We tentatively identify the observed absorption peaks as one-magnon and two-magnon transitions.

2 Details of Goethite Structure

The overall structure of goethite involves ribbons formed from paired linear chains of distorted octahedral $FeO_3(OH)_3^{6-}$ clusters. Looking down the ribbon axis, the ribbons share oxygens at four corners, forming a matrix that is roughly 50% open [1, 18].

The magnetic ordering of goethite has a fairly complex antiferromagnetic structure. The axis of antiferromagnetic alignment (c-axis) is nominally orthogonal to the ribbon axis. Results from Mössbauer spectroscopy on goethite powder suggest four magnetic sublattices due to two slightly different subsets of the four Fe^{3+} ions populating the goethite unit cell [8, 9, 19]. Roughly speaking, the spins lay parallel or antiparallel to the c-axis, but within each $+c$-directed or $-$c-directed subset of two spins, the spins tilt approximately 13° from the c-axis in opposite directions [8].

In some canted antiferromagnets, the canting results in a weak net moment. Although spin canting has been reported in goethite, inelastic neutron scattering has found little evidence of uniform spin canting in the anti-aligned spins that would identify goethite unequivocally as a "weak ferromagnet" [3, 8], as hematite was found to be [20]. Ozdemir and Dunlop, as well as Hedley, found weak ferromagnetism only along the antiferromagnetic spin axis [2, 21], suggesting a spin imbalance along this axis, but no spin canting off this axis. Van Oosterhout reported large variability in magnetic susceptibility and dehydration temperature as a function of how he synthesized acicular goethite crystallite samples, and their brief thermal aging, compared to the stable results that he observed in a goethite mineral crystal [22]. Since we have tested a comparable goethite mineral crystal, we expect our observations to be free of such underlying variations. However, such variability could arise in field conditions, and so is addressed below in Sect. 6: NDE application.

3 Experimental Methods

Several slices of natural polycrystalline goethite, cut using a diamond saw and then polished, were used in our study. The composition and the crystallite size of the goethite crystal were characterized using an X-ray diffraction method. Absorption

spectra of the goethite sample were obtained between 0.045 and 1.5 THz (1.5 and 50 cm^{-1}) for temperatures between 4.2 and 425 K using an experimental setup described previously [10]. The frequency of an AFMR transition is known to change rapidly when temperature is increased close to T_N, the magnetic phase transition from antiferromagnetic to superparamagnetic that is designated the Néel transition temperature. We use the baseline sections of spectra obtained at different temperatures to normalize the regions where absorption occurs, as in the previous hematite study [10]. Since this method does not require sample repositioning relative to the THz beam to normalize to the instrument power in the absence of absorption, this approach significantly reduces the baseline variations that result from standing wave interference patterns that are especially prevalent with high-index materials such as goethite [23].

Broadly tunable continuous-wave (CW) THz radiation was generated using an ErAs-GaAs photomixer [24]. This photomixer mixes the output from a fixed-frequency single-mode ring laser, operating near 356.4 THz (11,880 cm^{-1}), with the tunable output from a single-mode diode laser. Each of the two lasers has a line width less than 1 MHz and is focused onto the photomixer, driving the antenna structure at the difference frequency. The resulting THz radiation is first collimated by a Si lens and then focused by two off-axis parabolic mirrors (OAPs) onto the sample. The sample assembly is fixed to the cold finger of a liquid nitrogen/liquid helium-cooled cryostat located in the sample chamber. The transmitted power is focused onto a liquid helium-cooled bolometer using two OAPs and detected using a 480 Hz amplitude modulation method.

A superconducting quantum interference device [25] (SQUID) magnetometer was used to measure the Néel temperature (T_N) of the goethite crystal. The sample was loaded into a screw-sealed polytrifluorochloroethylene (PCTFE) sample holder for the magnetic measurements.

4 Results and Analysis

4.1 THz Spectra

As the optical excitation frequency was scanned between 0.045 and 1.5 THz (1.5 and 50 cm^{-1}), we observed two absorption peaks for our polycrystalline goethite sample across a temperature range covering its antiferromagnetic state. An example of the absorption data up to 33 cm^{-1} (1 THz) is shown in Fig. 1. As discussed above, the data are processed as a ratio in transmission at two different temperatures to minimize standing wave interference effects. This method results in both positive and negative going absorption peaks as illustrated in Fig. 1. Since the sample was large with respect to the average crystallite size (see Sect. 4.2), so that there were many crystallites randomly oriented, we expect that there would be no effect of polarization of the exciting wave on the results. With the sample held at 4.2 K, we observed absorptions at 0.57 THz (19 cm^{-1}) and 1.14 THz (38 cm^{-1}). These peaks were much broader than the hematite peaks that we observed earlier [1]. Each absorption was fit to a Lorentzian function to obtain the center frequencies as

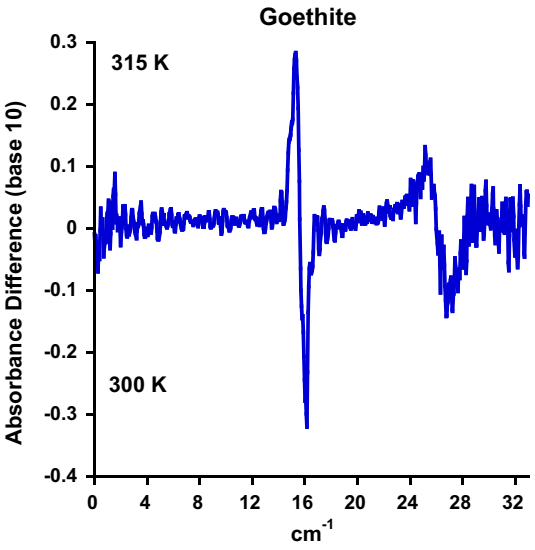

Fig. 1 Absorption data taken at 315 K shown relative to the absorption data taken at 300 K. The ratio is performed using the transmission spectra at these two temperatures. The shift of the two AFM resonances at the two different temperatures gives rise to the derivative like signals. The baseline is nearly devoid of standing wave interference effects since the sample has not been moved or replaced as is normally done when the ratio is performed against a blank

measurements were stepped across the range in temperature from 4.2 to 425 K. The resulting temperature dependence of the two center frequencies are shown in Fig. 2. There is a slight kink in the plot for the second peak that ranges from 240 to 320 K as shown in Fig. 2 and we discuss the possible origin of this kink in Sect. 5.

4.2 Crystallite Size Dependence of T_N

The Néel transition temperature, T_N, is known to vary with the crystallite size in polycrystalline samples. A linear relationship between T_N and inverse crystallite dimension, *d,* has been observed [17]: $T_N \approx \beta\ d^{-1}$, with a constant of proportionality $\beta = -1060 \pm 130$ K nm. So the value of T_N may prove useful as a technique to detect corrosion granularity at temperatures between ~300 and 425 K. Since we had a large and uniform polycrystal, we were able to add a maximal Néel transition temperature point to the plot presented in [17], and repeated this plot as Fig. 3. This reduction in T_N as particle size dwindles is attributed to the accentuated influence of surface states, including vacancies and defects, over bulk magnetics. The sample characterized in this present study had a mean crystallite size of 176 ± 20 nm as determined from profile fitting of the X-ray [111] diffraction peak and using a portion of the same polycrystalline sample that was used for the optical absorption measurements. Our measured value of T_N was 435 ± 1 K, which is close to the maximum Néel transition temperature recorded for a synthetic goethite sample of 440 K [22]. In Fig. 3, we revised the linear regression fit to include this maximal T_N point. From the extrapolation of our new linear fit, the T_N for bulk goethite with infinitely large crystallite size is estimated to be 417 ± 7 K and the constant of proportionality, β, is determined to be -1376 ± 168 K nm. The fact that 417 K is 4% less than the measured value of 435 K is another indication of the uncertainty in the fitted slope. However, the extrapolated infinitely large crystallite size value of

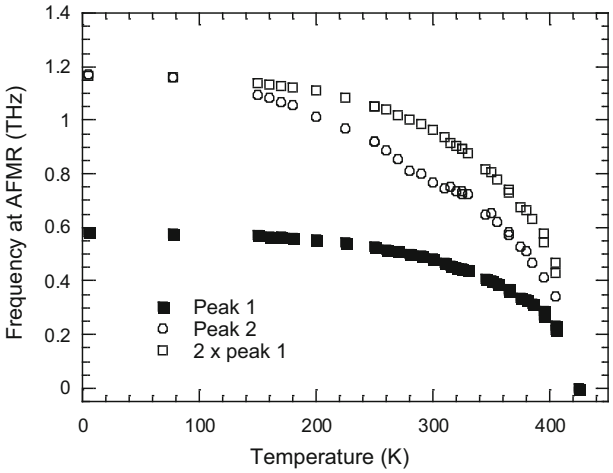

Fig. 2 Temperature dependence of the goethite AFMR transition measured using the THz spectrometer. The data point at T_N was obtained using a SQUID magnetometer. The *uncertainty bars* for the data were approximately the size of the data points, so are not shown. The uncertainty expressed in temperature dimension is type B, with coverage factor $k = 1$ (or 1 standard deviation [33]). The uncertainty expressed in the frequency dimension is type A, with coverage factor $k = 1$ (or 1 standard deviation [33])

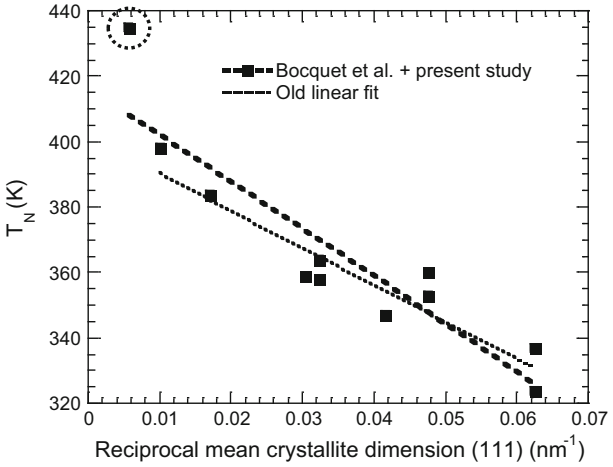

Fig. 3 T_N versus reciprocal mean crystallite [111] dimension for the goethite sample used in this study along with the data reported by Bocquet et al. [17]. The uncertainty expressed in crystallite dimension is type B, with coverage factor $k = 1$ (or 1 standard deviation [33]). The *uncertainty bars* for the data were approximately the size of the data points, so are not shown. Both the linear fit by Bocquet and the new linear fit, which includes the additional data point measured in this paper (outlined with a dashed circle), are shown

T_N for the new relation is closer to the measured value, 435 K, than the old linear extrapolation [17] of $T_N = 400$ K in this limit (see Fig. 3), or 8% below our measured value.

5 Discussion

The octahedral iron cluster, $(FeO_6)^{9-}$, has formed the basis for ferrite technical materials [26], and AFMR results recorded for such materials are comparable to our absorptions found here and for hematite [10]. Modern approaches are just beginning to reveal the complex anisotropy and symmetry of goethite magnetism at the unit cell level that relate to its magnon absorptions [27]. We have found two such resonant absorption peaks for this four magnetic sublattice structure.

We find that the lower resonance frequency compares favorably with reported spin-flop fields for goethite. In a simple two-sublattice model, the spin-flop transition fields B_{SF} and the antiferromagnetic resonance frequencies f_{AFMR} are related by $f_{AFMR} = \gamma B_{SF}$, where γ is the gyromagnetic ratio, approximately 28 GHz/T. The reported goethite spin-flop field of 20 Tesla (T) [8], translates to an AFMR frequency at 560 GHz, which compares well with our current result of 570 GHz at low temperature. Spin flop results clearly support the hypothesis that the lower frequency absorption is a single-magnon absorption. Similarly, the spin-flop field for crystal hematite 6.78 T [28] conservatively estimated a low-temperature AFMR of 190 GHz versus our previous result of 210 GHz.

We tentatively identify the upper resonance as a two-magnon absorption, although there are problems with this identification as we will note below. Two-magnon absorption involves electric dipole excitation of counter-propagating magnon pairs [29]. While the mechanism is effective for all wavevectors, the magnon density of states typically peaks at the Brillouin zone edge and other high symmetry points of the Brillouin zone, yielding broad two-magnon peaks that often have greater integrated intensity than the single-magnon peak. Our average line width (full width at half maximum) of absorptions in the low-frequency peak is approximately 26 GHz (0.86 cm^{-1}) and that of the high-frequency series is approximately 111 GHz (3.7 cm^{-1}). The integrated intensity for these upper peaks is roughly four times larger than the lower. The comparatively large integrated intensity and line width support two-magnon absorption for the upper peak.

A problem with the two-magnon identification stems from the fact that our upper resonance frequency is slightly *less* than a factor of two above the lower resonance frequency at higher temperature (>120 K), as accentuated in Fig. 4. According to two-magnon theory, the frequency of the two-magnon peak is twice the frequency of the zone edge magnons, so if we interpret the two peaks as one magnon (zone-center) and two-magnon (2 × zone edge) peaks, the peak frequencies imply that the zone edge magnon is actually at a slightly *lower* frequency than the zone-center magnon. Such a result is not expected for a simple Heisenberg antiferromagnet. In the low-temperature range (<100 K), the frequency of the higher energy peak is exactly twice of the lower frequency zone-center magnon. This observation is potentially consistent with an alternative scenario that two zone-center magnons are being absorbed simultaneously. However, additional theoretical work will be needed to more systematically understand the absorption cross section associated with the different mechanisms contributing to the observed multi-magnon transitions.

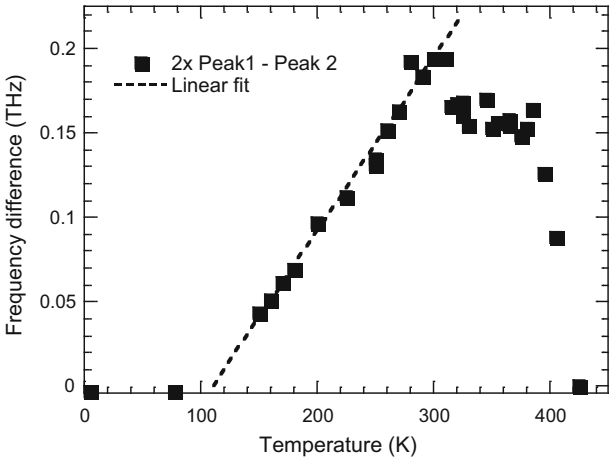

Fig. 4 Difference between twice the frequency of Peak 1 and the frequency of Peak 2, plotted as a function of temperature. The *uncertainty bars* for the data were approximately the size of the data points, so are not shown

In addition, we also note that a similar result has been reported from a low-temperature, far-infrared study on cobalt carbonate ($CoCO_3$, $T_N \approx 18.1$ K). A lower frequency absorption line at 1.03 THz (34.6 cm^{-1}) was identified as single magnon and one at 1.64 THz (54.7 cm^{-1}) as two magnon [30]. The latter was identified based on its much longer tail above T_N that is indicative of two-magnon absorption [29]. This absorption was also several times broader and had the asymmetrical shape that is characteristic of zone edge absorption.

To this point, we have interpreted the spectra by comparison to antiferromagnet models involving two sublattices, and we now hypothesize how the four-sublattice magnetic structure of goethite [8, 9] may play a significant role. For resonances at the zone center, each uniformly precessing sublattice of spins may be represented by a single spin. In general, a four-spin system will have more resonances than a two-spin system, and it is plausible that moving from a two-sublattice system to a four-sublattice system may produce splitting of the one-magnon peak.

The kink between 240 and 320 K in the upper frequency peak of Fig. 2 may be the result of a partial magnetic structural rearrangement. Results from differential scanning calorimetry on five different goethite mineral crystals do show a small endothermic peak indicative of a partial structural rearrangement in going from 240 to 320 K [31].

6 NDE Application

In applying these results and further developing this experimental technique as an NDE method, detecting the one-magnon antiferromagnetic transition usually means just seeing the amplitude of the peak above any noise. Since, very roughly speaking, the integrated intensity of a peak is proportional to the amplitude times the line

width, this means that the peak amplitudes of the upper peak series are about the same as that of the lower frequency peak. Therefore, in the absence of significant baseline variations, both resonances should be about equally detectable and could both serve as an NDE indication of the presence of goethite corrosion.

The proposed NDE method would use the method of ratioing at different temperatures, which implies a need to be able to control the temperature of the system being analyzed. The frequency at which the AFM transition would be observed depends on the relation of the ambient temperature to the Néel temperature, which can vary with crystallite size. The empirical relation given in this paper, based on new data from this paper and on previous work, would help with this analysis. In general, we would expect that in detecting goethite corrosion in cases where the crystallite size was smaller, the results of Fig. 2 would simply rescale to accommodate a smaller value of T_N. However, the peaks shown in Fig. 1 would probably broaden and be noisier and, therefore, be somewhat harder to identify. In reference to this, we previously applied the same measurement technique to a steel plate in reflection mode at room temperature that was covered with thin film of rust [32]. The rust was formed in an open outdoor environment so the composition of the rust was most likely goethite. Broad but strong peaks with 98% fraction absorption were clearly seen having peak centers nicely corresponding to those observed here at room temperature. This suggests the field detection of surface corrosion using AFMR of goethite may indeed be practical.

The frequencies presented in Fig. 2 limit the application of Terahertz waves to identify goethite corrosion through significant thicknesses of materials such as concrete, which has high attenuation. Furthermore, the high- and low-frequency linewidths overlap and coalesce as temperature is increased to T_N, so field measurements should be made below this temperature. One application might be to detecting corrosion under insulation in pipe systems in factories. Cold pipes should present no problem, but any goethite corrosion on a pipe that is at a temperature over or around 400 K (e.g., a high-pressure steam pipe) would not be detectable by this method, since the goethite is not antiferromagnetic above the Néel temperature.

7 Summary

We report high-resolution optical absorption measurements between 0.045 and 1.5 THz (1.5 and 50 cm^{-1}) in antiferromagnetic goethite (FeOOH), observing two peaks that we tentatively identify as one-magnon and two-magnon transitions. These are measured over a range of temperatures from 4.2 to 425 K, using a method of spectral ratioing between two nearby temperatures. These resonances in the THz region make possible a method for the early detection of goethite formation on iron covered with polymeric or other protective coatings (e.g., pipe insulation) since these latter materials are largely transparent in the THz region. We have also extended the crystallite size dependence of the Néel temperature for goethite, which may be of use for employing these results as a field NDE method.

Acknowledgements S. G. C. gratefully acknowledges useful discussions with J. R. Simpson. This article reflects the views of the author and should not be construed to represent FDA's views or policies. The work was supported by the NIST Innovations in Measurement Science research program entitled "Detection of Corrosion in Steel-Reinforced Concrete by Antiferromagnetic Resonance". All the authors would like to pay tribute to William Egelhoff (deceased) who was the originator of the idea of using AFMR detection of certain iron corrosion products as a means of detecting early corrosion of steel under protective layers.

References

1. R.M. Cornell, U. Schwertmann, *The Iron Oxides, Structure, Properties, Reactions, Occurrences, and Uses* (Wiley-VCH, Weinheim, 2003)
2. O. Ozdemir, D.J. Dunlop, Geophys. Res. Lett. **23**(9), 921–924 (1996)
3. F. Martin-Hernandez, M.M. Garcia-Hernandez, Geophys. J. Int. **181**, 756–761 (2010)
4. S.J. Oh, D. C. Cook, H. E. Townsend, Hyperfine Interact. **112**(1–4), 59–66, 12 (1998)
5. K.E. Garcia, A.L. Morales, C.A. Barrero, J.M. Greneche, Corros. Sci. **48**, 2813–2830 (2006)
6. E. Zepeda-Alarcon, H. Nakotte, A.F. Gualtieri, G. King, K. Page, S.C. Vogel, H.-W. Wang, H.-R. Wenk, J. Appl. Crystallogr. **47**, 1983–1991 (2014)
7. A. Szytula, A. Burewicz, Z. Dimitrijevic, S. Krasnicki, H. Rzany, J. Todorovic, A. Wanic, W. Wolski, Physica Status Solidi **26**, 429–434 (1968)
8. J.M.D. Coey, A. Barry, J.-M. Brotto, H. Rakoto, S. Brennan, W.N. Mussel, A. Collomb, D. Fruchart, J. Phys. Condens. Matter **7**, 759–768 (1995)
9. J.B. Forsyth, I.G. Hedley, C.E. Johnson, J. Phys. C **1**, 179–187 (1968)
10. S.G. Chou, P.E. Stutzman, S. Wang, E.J. Garboczi, W.F. Egelhoff, D.F. Plusquellic, J. Phys. Chem. C **116**, 16161 (2012)
11. V.S. Agarwala, P.L. Reed, S. Ahmad, in *Proceedings of CORROSION 2000*, 26–31 March (NACE International, Orlando, Florida, 2000)
12. D.J. Duquette, R.E. Schafrik, A.I. Asphahani, G.P. Bierwagen, D.P. Butt, G.S. Frankel, R.C. Newman, S.N. Rosenbloom, L.H. Schwartz, J.R. Scully, P.F. Tortorelli, D. Trejo, D.F. Untereker, M. Urquidi-Macdonald, *Research Opportunities in Corrosion Science and Engineering* (National Academies Press, Washington, DC, 2011)
13. G.H. Koch, M.P. Brongers, N.G. Thompson, Y.P. Virmani, J.H. Payer, *Corrosion Cost and Preventive Strategies in the United States*, Federal Highway Administration Report FHWA-RD-01-156, R315-01. https://trid.trb.org/view.aspx?id=707382 (2002)
14. N. R. C. Committee on Research Opportunities in Corrosion Science and Engineering, *Research Opportunities in Corrosion Science and Engineering* (National Academy Press, Washington, DC, 2011)
15. G.-L. Song, Front. Mater. Res. **1**, 1–3 (2014)
16. H.W. Song, V. Saraswathy, Int. J. Electrochem. Sci. **2**, 1–28 (2007)
17. S. Bocquet, R.J. Pollard, J.D. Cashion, Phys. Rev. B **46**(18), 11657–11664 (1992)
18. S.K. Ghose, G.A. Waychunas, T.P. Trainor, P.J. Eng, Geochim. Cosmochim. Acta **74**, 1943–1953 (2010)
19. A.Z. Hrynkiewicz, D.S. Kulgawczuk, K. Tomala, Phys. Lett. **17**(2), 93–95 (1965)
20. L. Néel, Rev. Mod. Phys. **25**(1), 58–63 (1953)
21. I.G. Hedley, Z. Geophys. **37**, 409–420 (1971)
22. G.W. van Oosterhout, in *Proceedings International Conference on Magnetism, Nottingham, 1964* (Physical Society, London, 1965), pp. 529–532
23. R.D. Shannon, R.C. Shannon, O. Medenbach, R.X. Fischer, J. Phys. Chem. Ref. Data **31**(4), 931–970 (2002)
24. E.R. Brown, K.A. McIntosh, K.B. Nichols, C.L. Dennis, Appl. Phys. Lett. **66**(3), 285–287 (1995)
25. V. Provenzano, B. Baumgold, R.D. Shull, A.J. Shapiro, K. Koyama, K. Watanabe, N.K. Singh, K.G. Suresh, A.K. Nigam, S.K. Malik, J. Appl. Phys. **99**(8), 08K906 (2006). doi:10.1063/1.2159396
26. G.F. Dionne, *Magnetic Oxides* (Springer, New York, 2009)
27. V.E. Dmitrienko, E.N. Ovhinnikova, J. Kokubun, K. Ishida, JETP Lett. **92**(6), 383–387 (2010)
28. P.J. Besser, A.H. Morrish, Phys. Lett. **13**(4), 289–290 (1964)
29. M.G. Cottam, D.J. Lockwood, *Light Scattering in Magnetic Solids* (Wiley, New York, 1986)

30. V.M. Naumenko, V.V. Eremenko, A.I. Maslennikov, A.V. Kovalenko, JETP Lett. **27**(1), 17–20 (1978)
31. M.J. Dekkers, Geophys. J. Int. **103**, 233–250 (1990)
32. D.F. Plusquellic, V. Provenzano, S.G. Chou, in *MRS Proceedings*, Boston, vol. 1296 (Cambridge University Press, Cambridge, 2010). doi:10.1557/opl.2011.1443
33. B.N. Taylor, C.E. Kuyatt, *Guidelines for Evaluating and Expressing the Uncertainty of NIST Measurement Results*. NIST Technical Note 1297 (NIST, Gaithersburg, 1994). http://physics.nist.gov/Pubs/guidelines/contents.html